Research Article

Cancer Prevention Research

Targeting p53-Null Neuroblastomas through RLIP76

Jyotsana Singhal, Sushma Yadav, Lokesh Dalasanur Nagaprashantha, Rit Vatsyayan, Sharad S. Singhal, and Sanjay Awasthi

Abstract

The search for p53-independent mechanism of cancer cell killing is highly relevant to pediatric neuroblastomas, where successful therapy is limited by its transformation into p53-mutant and a highly drug-resistant neoplasm. Our studies on the drug-resistant p53-mutant as compared with drug-resistant p53 wild-type neuroblastoma revealed a novel mechanism for resistance to apoptosis: a direct role of p53 in regulating the cellular concentration of proapoptotic alkenals by functioning as a specific and saturable allosteric inhibitor of the alkenal–glutathione conjugate transporter, RLIP76. The RLIP76-p53 complex was showed by both immunoprecipitation analyses of purified proteins and immunofluorescence analysis. Drug transport studies revealed that p53 inhibited both basal and PKCα-stimulated transport of glutathione conjugates of 4HNE (GSHNE) and doxorubicin. Drug resistance was significantly greater for p53-mutant as compared with p53 wild-type neuroblastoma cell lines, but both were susceptible to depletion of RLIP76 by antisense alone. In addition, inhibition of RLIP76 significantly enhanced the cytotoxicity of cisplatin. Taken together, these studies provide powerful evidence for a novel mechanism for drug and apoptosis resistance in p53-mutant neuroblastoma, based on a model of regulation of p53-induced apoptosis by RLIP76, where p53 is a saturable and specific allosteric inhibitor of RLIP76, and p53 loss results in overexpression of RLIP76; thus, in the absence of p53, the drug and glutathione-conjugate transport activities of RLIP76 are enhanced. Most importantly, our findings strongly indicate RLIP76 as a novel target for therapy of drug-resistant and p53-mutant neuroblastoma. *Cancer Prev Res; 4(6); 879–89. ©2011 AACR.*

Introduction

Neuroblastomas are the most common solid tumors in infants and represent the third most common class of pediatric malignancies (1). Neuroblastomas arise from the neural crest tissue of the sympathetic ganglia. Neuroblastomas can metastasize to the liver where the metastatic tumors can be massive (2). The most common metastatic site is the skull where it metastasizes to sphenoid bone and retro bulbar tissue leading to common symptoms of proptosis and periorbital echymosis (3, 4). Surgical resection of localized neuroblastomas offers good clinical remission but advanced stages of neuroblastomas require aggressive multimodality treatment (1, 5, 6). The other treatment modalities currently being investigated in refractory and relapsed neuroblastomas include antiangiogenic drugs and fenretinide, a retinoid derivative (7, 8). Given the limited 3-year event-free survival of 15% in the incident population and the nature of symptoms in affected children, validation of novel drug targets becomes a vital focus of translational research to achieve complete therapeutic response in multidrug-resistant neuroblastomas (9–11).

The tumor suppressor p53 plays a significant role in multidrug resistance of neuroblastomas. Though the p53 mutations are relatively rare in primary neuroblastomas, advanced neuroblastomas acquire loss-of-function mutations in p53, which render them resistant to conventional chemotherapeutic regimens (12–14). It is an established fact that p53 mediates the induction of apoptosis in cells treated with chemotherapeutic drugs and loss-of-function mutations in p53 are associated with resistance to both anticancer drugs and radiation therapy (15, 16). The use of chemotherapeutic drugs such as cisplatin (CDDP), doxorubicin (DOX), and vincristine is highly limited in refractory and relapsed neuroblastomas due to frequent loss-of-function mutations in the tumor suppressor p53 (17, 18).

The human ral-binding protein 1(RALBP1 or RLIP76) is a 76 kDa multifunctional drug transport protein with substrate-stimulated ATPase activity and overexpressed in majority of cancers such as cancers of the lung, colon, kidney, melanoma, ovary, prostate, and breast (19, 20). Normally, RLIP76 functions as an antiapoptotic and stress-protective protein that prevents accumulation of oxidative-stress–induced toxic metabolites inside the

Authors' Affiliation: Department of Molecular Biology and Immunology, University of North Texas Health Science Center, Fort Worth, Texas

Corresponding Author: Sharad Singhal, University of North Texas Health Science Center, Fort Worth, TX 76107-2699. Phone: 817-735-0459; Fax: 817-735-2118. E-mail: sharad.singhal@unthsc.edu or Sanjay Awasthi, City of Hope, Beckman Research Institute, Duarte, CA 91010. Phone: 626-256-4673; Fax: 626-471-9374. E-mail: sawasthi@coh.org

doi: 10.1158/1940-6207.CAPR-11-0025

cells. RLIP76 acts by catalyzing the ATP-dependent efflux of glutathione–electrophile conjugates (GS-E) of lipid peroxidation products (19). In the previous studies, we have shown that the inhibition of RLIP76 by antisense-induced selective apoptosis in several cell lines of lung, prostate, kidney, colon, and breast cancers (19, 20). The hallmark of inhibition of RLIP76 in our previous tumor models of various cancers has been selective toxicity toward targeted tumor cells sparing normal cells.

Until today, the investigations into the mechanisms of p53-induced apoptosis in neuroblastoma have been focused on the inhibition of cell cycle checkpoints on DNA damage and induction of the transcription of apoptotic proteins such as bax, bak, and PUMA on cytotoxic stimuli to cells (21). The nonnuclear and transcription-independent mechanisms of p53-mediated cell death include stimulation of caspase 3 activation by mitochondrial translocation of p53 on exposure to radiation (22). In this study, we investigated the interaction of p53 on the multidrug transporter RLIP76 followed by the analysis of the impact of RLIP76 inhibition in targeting multidrug-resistant neuroblastoma. We used 2 p53 wild-type (SMS-KCNR and LAN-5) and 2 p53-mutant (CHLA-90 and SKN-BE2) neuroblastoma cell lines for our studies. CHLA-90 is a neuroblastoma cell line derived at progressive stage of neuroblastoma following multiagent chemotherapy and SKN-BE2 is derived from recurrent neuroblastoma. Neuroblastomas established as cell lines following acquisition of drug resistance during multidrug therapy and maintained without exposure to drugs during regular cultures still retain the properties of specific drug resistance that was acquired during initial multidrug chemotherapy (23). Thus, the neuroblastoma cell lines with mutant p53 were relevant to specifically study the loss-of-p53–induced drug resistance in neuroblastoma.

Materials and Methods

Reagents

Doxorubicin was obtained from Adria Laboratories. Cisplatin was obtained from Bristol–Meyers Squibb. Source of polyclonal rabbit anti-human rec-RLIP76 antibodies was same as previously described (24). P53 antibodies were purchased from Santa Cruz Biotechnology. Maxfect transfection reagent was from MoleculA. PKCα was obtained from Molecular Probes. 4-Hydroxynonenal (4HNE) and malondialdehyde (MDA) measurements kit was purchased from Oxis International. Gene-specific primers, scrambled as well as RLIP76 antisense were purchased from Biosynthesis Inc. Radiolabeled ^{3}H-GSHNE (specific activity, 3.1×10^{4} cpm/nmol) was synthesized as described by us previously (25). ^{14}C-DOX (specific activity, 54 mCi/mmol) was purchased from Amersham Corporation.

Cell lines

CHLA-90 and SKN-BE2 (p53-mutant) cell lines have been established from tumors obtained from patients who had relapsed after intensive multiagent myeloablative chemoradiotherapy and bone-marrow transplantation. SMS-KCNR and LAN-5 (p53 wild-type) cell lines have been established from tumors obtained from neuroblastoma patients. Human neuroblastoma cell lines were kindly authenticated and provided in May 2010 by Dr. Patrick Reynolds, MD PhD, Children's Neuroblastoma Cancer Foundation/Children Oncology group, Texas Tech University, Department of Cell Biology & Biochemistry, School of Medicine, Lubbock, TX. The cells were tested for *Mycoplasma* once at the beginning immediately after receiving the cell lines and after 3 months. All the experiments were conducted within 5 months of securing the cell lines. Cells were grown in complete medium consisting of Iscove's modified Dulbecco's medium supplemented with 3 mmol/L L-glutamine, 5 μg/mL each of insulin and transferrin, 5 ng/mL of selenous acid (ITS culture supplement), and 20% FBS at 37°C in a humidified 5% CO_2 atmosphere. Cell lines were subcultured by detaching without trypsin from culture plates by using a modified Puck's Solution A plus EDTA (Puck's EDTA) which contain 140 mmol/L NaCl, 5 mmol/L KCl, 5.5 mmol/L glucose, 4 mmol/L $NaHCO_3$, 0.8 mmol/L EDTA, 13 μmol/L phenol red, and 9 mmol/L HEPES buffer (pH 7.3).

Cross-linking and immunoprecipitation

The protein–protein cross-linking and immunoprecipitation assay was carried out according to the method of Aumais and colleagues (26). Briefly, purified rec-RLIP76 and p53 (10 μg each) were cross-linked by incubation with 0.1 mmol/L N-succinimidyl 3-(2-pyridyldithio) propionate (SPDP; Sigma) in a total volume of 0.5 mL in 10 mmol/L sodium phosphate buffer, pH 7.4, for 30 minutes. Excess SPDP was removed by passing the solution through a Sephadex G-50 spin column pre-equilibrated with sodium phosphate buffer (pH 7.4). The samples were treated with 0.5 mmol/L N-ethylmaleimide for 10 minutes to block all free SH groups that could prematurely cleave cross-links. Protein complexes were immune-precipitated by incubating with either preimmune immunoglobulin G (IgG) or anti-RLIP76 IgG for 12 hours followed by with protein A-Sepharose (20 μL of 50% bead slurry) in radioimmunoprecipitation assay buffer [50 mmol/L Tris-HCl (pH 7.4), 4 mmol/L EDTA, 150 mmol/L NaCl, 1% Triton X-100, and 0.1% SDS] for 2 hours. Samples were sedimented by centrifugation at 10,000 × *g*, washed 3 times with radioimmunoprecipitation assay buffer, and then resuspended in 100 μL of SDS-PAGE sample buffer. To check the effect of PKCα in the interaction of RLIP76-p53, the immunoprecipitation was carried out in the presence of equimolar concentration of PKCα in the absence and presence of 1 mmol/L ATP. The reaction mixture was incubated for 30 minutes at 37°C and the cross-linking and immunoprecipitation was carried out as described earlier. Samples were analyzed by SDS-PAGE and Western blotting against anti-RLIP76, anti-PKCα, and anti-p53 IgG.

4HNE and MDA levels

Measurement of endogenous levels of 4HNE and MDA in a panel of neuroblastoma cells were carried out spectrophotometrically by using the LPO 586 measurement kit (Oxis International) according to manufacturer's instructions.

Drug sensitivity assay

Cell density measurements were done by a hemacytometer to count dye-excluding cells resistant to staining with trypan blue. Approximately 2×10^4 cells were plated into each well of a 96-well flat-bottomed microtiter plate 24 hours prior to addition of medium containing varying concentrations of antibodies or drugs. After 24 hours of incubation, 40 μL aliquots of drugs (DOX and CDDP) diluted in medium were added to get final concentration between 0.001 and 100 μmol/L to 8 replicate wells. After 96 hours of incubation, 20 μL (5mg/mL stock) MTT was added to each well and incubated for 2 hours at 37°C. The plates were centrifuged and medium was removed. Formazan dye trapped in cells was dissolved by addition of 100 μL dimethylsulfoxide with gentle shaking for 2 hours at room temperature, followed by measurement of absorbance at 570 nm. Depletion of RLIP76 expression in cells by RLIP76 antisense was measured as follows: cells were incubated for 6 hours with 0 to 10 μg/mL RLIP76 antisense in Maxfect transfection reagent (MoleculA) according to the manufacturer-provided protocol.

Liposome preparation

The proteoliposome preparation procedures used here have been validated and described in detail previously (24, 27). Briefly, proteoliposomes containing RLIP76 or p53 were prepared by addition of the purified recombinant protein to a sonicated emulsion of 1:4 cholesterol and phospholipids (soybean asolectin, 95% purity; Sigma Chemicals Co.) in liposome reconstitution buffer [10 mmol/L Tris-HCl (pH 7.4), 2 mmol/L $MgCl_2$, 1 mmol/L EGTA, 100 mmol/L KCl, 40 mmol/L sucrose, 2.8 mmol/L BME, 0.05 mmol/L BHT, and 0.025% polidocanol]. Liposome formation was initiated by addition of SM2 Biobeads (200 mg/mL). We have shown that vesiculation is complete within 4 hours and yields primarily unilammelar vesicles with median diameter of 0.25 μm and intravesicular/extravesicular volume ratio of 18 μL/mL (24). The control liposomes or the liposomes reconstituted with purified RLIP76 were used for transfecting cells in culture. Efficiency of delivery for RLIP76 proteoliposomes has been established previously (24).

Radiation protection by RLIP76 liposomal delivery

A total of 2.5×10^3 CHLA-90 and SMS-KCNR cells were treated with control liposome and RLIP76 proteoliposomes (50 μg/mL final conc.) for 24 hours prior to radiation at 100 to 500 cGy by using a Varian Clinac linear accelerator (2100 C; 6-MeV photon beams) at the Texas Cancer Center, Arlington, TX. Cells were inoculated into colony-forming assays immediately after radiation. After 7 days, colonies were stained with methylene blue and counted by using an image acquisition and analysis system (Innotech Alpha Imager HP). The results presented are the mean and SD from 3 separate experiments. Please note that CHLA-90 (6,255 colonies/mL); and SMS-KCNR (6,620 colonies/mL); plating efficiency of CHLA-90 and SMS-KCNR are 1 and 1.06, respectively. After RLIP76 proteoliposomes treatment; CHLA-90 (7,130 colonies/mL); and SMS-KCNR (7,035 colonies/mL); plating efficiency of CHLA-90 and SMS-KCNR after RLIP76 proteoliposomes treatment were 1.14 and 1.06, respectively.

Preparation of total crude fractions for Western blot analyses

Cells were pelleted and washed with balanced salt solution. Washed cells were lysed and sonicated for 30 seconds at 50 W and incubated for 4 hours at 4°C with occasional shaking. After incubation, the resultant preparation was centrifuged at 105,000 × *g* for 60 minutes at 4°C. The supernatant was collected and aliquots of crude fraction were applied to SDS-PAGE and Western blot analyses were carried out. Western blots were developed by enhanced chemiluminescence reagent (Pierce).

Immunocytochemistry for interaction of RLIP76 and p53

Colocalization of RLIP76 and p53 was carried out on neuroblastoma, LAN-5 (wild-type p53), and SKN-BE2 (mutant p53) fixed cells by method described previously with slight modifications (28). Briefly, cells were grown on glass coverslips and fixed with methanol and acetic acid (3:1). Nonspecific antibody interactions were minimized by pretreating the cells with 10% goat serum in TBS for 60 minutes at room temperature. The cells were subjected to immunocytochemistry by using anti-RLIP76 IgG (raised in rabbit) and anti-p53 IgG (raised in mice) as a primary antibody, and goat anti-rabbit rhodamine red-x conjugated (for RLIP76) or goat anti-mouse fluorescein isothiocyanate (FITC) conjugated (for p53) as secondary antibody. DAPI (4′,6-diamidino-2-phenylindole) was used as a nuclear counterstain. Slides were analyzed by confocal laser microscope (Leica TCS-SP5).

Depletion or inhibition of RLIP76 expression by RLIP76 antisense and antibody

Depletion of RLIP76 expression by RLIP76 antisense (2–10 μg/mL) was done by using Maxfect Transfection Reagent according to manufacturer's protocol. Briefly, cells were incubated for 6 hours with 2 to 10 μg/mL RLIP76 antisense, washed with PBS, followed by 48 hours of incubation at 37°C in medium. For inhibition of RLIP76, anti-RLIP76 IgG at a concentration of 10 to 20 μg/mL was used.

Transport of ^{14}C-DOX and ^{3}H-GSHNE by RLIP76 and its inhibition by p53

For these experiments, fixed amount of purified rec-RLIP76 (250 ng) was reconstituted into proteoliposomes

along with varying amounts (0–250 ng) of purified rec-p53, in the absence/presence of 12.5 ng of PKCα, 1 mmol/L ATP, and were incubated for 30 minutes at 37°C. Effect of PKCα-mediated phosphorylation on RLIP76-mediated ^{14}C-DOX and ^{3}H-GSHNE transports were measured as described (27, 29). In one control, p53 proteins were excluded whereas in another control equivalent amount of bovine serum albumin were reconstituted in proteoliposomes. Each determination was carried out in triplicate.

Animal model

Hsd:athymic nude nu/nu mice were obtained from Harlan. All animal experiments were carried out in accordance with a protocol approved by the Institutional Animal Care and Use Committee. Twenty 11-week-old male mice were divided into 4 groups of 5 animals (treated with preimmune serum, scrambled antisense DNA, anti-RLIP76 IgG, and RLIP76 antisense). All 20 animals were injected with 2×10^6 neuroblastoma cell (SMS-KCNR) suspensions in 100 μL of PBS, subcutaneously into 1 flank of each nu/nu nude mouse. Animals were examined daily for signs of tumor growth. Treatment was administered when the tumor surface area exceeded 40 mm^2 (~28 days). Treatment consisted of 200 μg of anti-RLIP76 IgG or antisense in 100 μL PBS, intraperitoneally (i.p.). Control groups were treated with 200 μg/100 μL preimmune serum or scrambled antisense DNA. Tumors were measured in 2 dimensions by using calipers.

Statistical analyses

All experiments were conducted in triplicates. The experimental data was statistically analyzed by 2-tailed unpaired Student's *t* test or by 1-way ANOVA and are expressed as the mean ± SD. A value of $P < 0.05$ was considered statistically significant.

Results

Multidrug resistance and expression of RLIP76 in p53-mutant neuroblastomas

We first compared the neuroblastoma cells expressing wild-type p53 and mutant p53 for multidrug resistance on treatment with chemotherapeutic drugs, DOX and CDDP. The CHLA-90 and SKN-BE2 cells with mutant p53 were more resistant for all the tested drugs than the SMS-KCNR and LAN-5 cells with wild-type p53. The IC_{50} values for DOX were 0.60 ± 0.1 μmol/L and 0.88 ± 0.1 μmol/L in CHLA-90 and SKN-BE2 p53-mutant cells, respectively, which were significantly higher by an order of magnitude of approximately 35-fold when compared with p53 wild-type neuroblastomas (IC_{50}: 0.02 ± 0.0 μmol/L). The IC_{50} values for CDDP were 30 ± 4 μmol/L and 22 ± 2 μmol/L in CHLA-90 and SKN-BE2 p53-mutant cells, respectively, which were significantly higher by order of magnitude of 3- to 7-fold when compared with p53 wild-type neuroblastomas (IC_{50}: 4 ± 1 μmol/L and 10 ± 1 in SMS-KCNR and LAN-5 cells, respectively; Table 1). P53 is one of the key regulators of antioxidant network of the cells and the interplay between reactive oxygen species (ROS) and p53 is complex (30). Wild-type p53 in response to stress and DNA damage in normal cells activates pro-oxidant genes leading to increased ROS and apoptosis of damaged cells. Wild-type p53 in nonstressed cells stimulates the transcription of antioxidant genes leading to reduced ROS and thus protects the ROS-induced mutations in genes (30). Thus, the neuroblastoma cells with mutant p53 in regular cultures should possibly differ in the oxidative stress. The level of end products of lipid peroxidation of 4HNE and MDA were substantially higher in p53-mutant neuroblastoma cells compared with wild-type p53 expressing neuroblastoma cells (Fig. 1A; $P < 0.001$). But, interestingly, the p53-mutant neuroblastomas with higher and toxic oxidative-stress markers such as 4HNE and MDA were resistant to apoptosis induction by chemotherapy drugs relative to neuroblastomas with wild-type p53. Thus, in addition to lack of p53 function in multidrug-resistant neuroblastomas, it indicated a possibility for upregulation of cellular defense against toxic end products of ROS. Hence, we studied the expression of RLIP76, a multispecific transporter of GS-E of lipid peroxidation and chemotherapy drugs. We observed that the expression of RLIP76 was significantly higher in p53-mutant as compared with p53 wild-type neuroblastomas (Fig. 1B). These findings indicate that the p53-mutant neuroblastomas might be dependent on the function of RLIP76 to buffer the enhanced oxidative stress. RLIP76 regulates the cellular concentration of products of lipid peroxidation. 4HNE, a marker of oxidative stress, has concentration-dependent effects in cells. Moderate levels of 4HNE stimulate proliferation whereas very high levels of 4HNE are toxic to even transformed and relatively apoptosis-resistant cancer cells (31). We observed that p53-mutant neuroblastoma cells have higher levels of 4HNE in spite of higher expression of the GSHNE transporter RLIP76. This could be attributed to activation of cyp2E1 in p53-mutant neuroblastomas, which enhances the generation of 4HNE from ω-6 fatty acids (32, 33). Thus, p53-mutant neuroblastomas have higher 4HNE relative to p53 wild-type cells, but they may not be able to reach very toxic concentrations due to RLIP76 overexpression. Thus, the "moderately high levels of 4HNE" attained due to a fine calibration between cyp2E1-mediated enhanced generation of 4HNE and RLIP76-mediated efflux could have stimulatory effect on cellular proliferative pathways.

To further confirm the protective effects of RLIP76 in neuroblastomas, we supplemented 1 p53-mutant (CHLA-90) and 1 p53 wild-type (SMS-KCNR) neuroblastoma cells with RLIP76 by liposomal delivery and tested the radiation sensitivity in relation to respective cell lines transfected with control liposomes. RLIP76 delivery protected both the cell lines from toxic oxidative stress induced on radiation exposure (Fig. 1C).

Table 1. P53 mutations and drug resistance in neuroblastoma cell lines

Status of p53	Cell line	p53 Mutation	IC_{50} (μmol/L)	
			DOX	CDDP
Mutated	CHLA90	E286K	0.60 ± 0.1	30 ± 4
	SK-N-BE(2)	C135F	0.88 ± 0.1	22 ± 2
Wild-type	SMS-KCNR		0.02 ± 0.0	4 ± 1
	LAN-5		0.02 ± 0.0	10 ± 1

NOTE: Drug sensitivity assays were carried out by MTT to determine IC_{50} values. The values are presented as mean ± SD from 3 separate determinations with 8 replicates each ($n = 24$).

Immunoprecipitation and immunocytochemistry analysis of the interaction of RLIP76 with p53

As RLIP76 was increased in p53-mutant neuroblastoma cell lines, we next investigated the functional status of RLIP76 in the presence or absence of p53. In this regard, we first analyzed whether p53 interacts with RLIP76 in the presence of equimolar concentrations of RLIP76 and PKCα, a known activator of RLIP76. Our previous studies have indicated that PKCα phosphorylates RLIP76 on S^{118}, T^{297}, S^{353}, and S^{509} (29). Hence, we wanted to study whether the PKCα-mediated phosphorylations have any impact on the binding assay. Immunoprecipitation studies revealed that RLIP76 binds with p53 both in the presence and absence of PKCα and that any phosphorylation by PKCα is not essential for the binding of p53 to RLIP76. But, the binding of p53 to RLIP76 was enhanced in the presence of PKCα and ATP (Fig. 2A, lane 5). Next, we analyzed the binding of p53 to RLIP76 in SKN-BE2 cells expressing mutant p53 and LAN-5 cells expressing wild-type p53. Immunocytochemistry for the binding of RLIP76 and p53 revealed enhanced p53 binding to RLIP76 in LAN-5 neuroblastoma cells relative to p53-mutant SKN-BE2 cells as revealed by an yellow overlay fluorescence when stained with fluorescent antibodies for RLIP76 (red, rhodamine) and p53 (green, FITC; Fig. 2B). Thus, the confirmation of enhanced binding of wild-type 53 over mutant p53 to RLIP76 further lead to investigation of the effect of p53 binding on RLIP76 transport function.

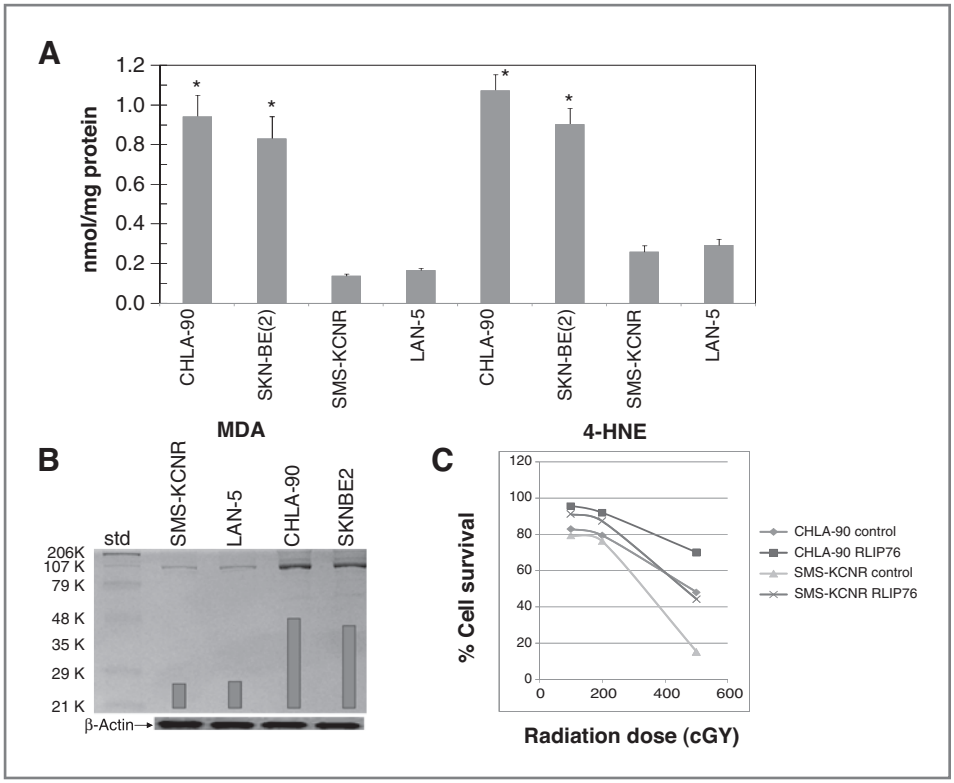

Figure 1. Measurement of endogenous levels of 4HNE and MDA in a panel of neuroblastoma cells (A; $P < 0.001$). Expression of RLIP76 in neuroblastoma cells as assessed by Western blot analyses by using anti-RLIP76 IgG as a primary antibodies. The bands were quantified by scanning densitometry by using Innotech Alpha Imager HP. β-Actin was used as a loading control (B). Protective effect of control liposome and RLIP76 proteoliposomes (50 μg/mL) on radiation toxicity by colony-forming assay (C; $P < 0.01$). A and C, results are average and SD from 3 separate experiments, each in triplicates ($n = 9$).

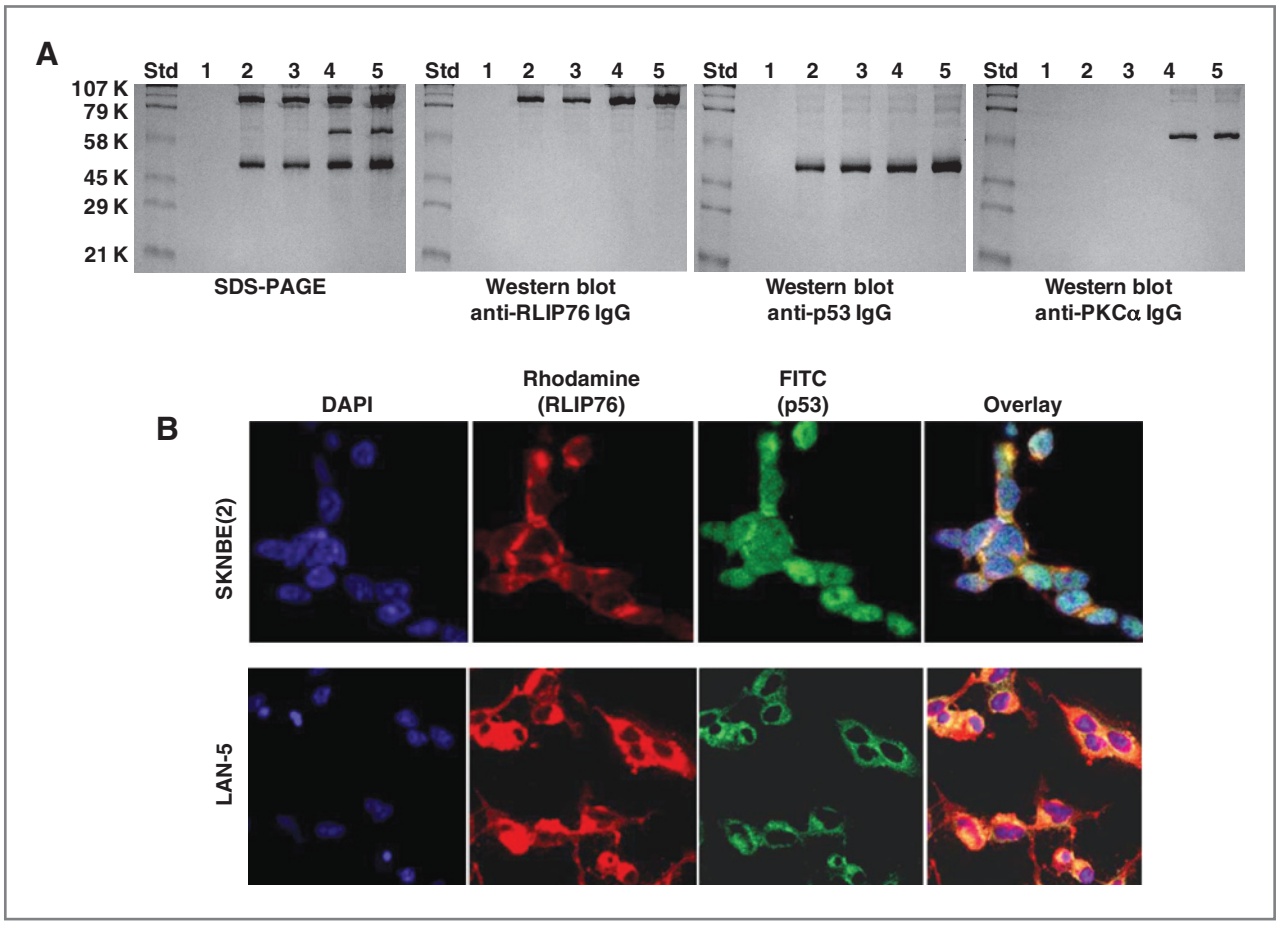

Figure 2. Interaction of RLIP76 with p53. Purified rec-RLIP76 and p53 proteins (10 μg each), in the absence/presence of equimolar concentration of PKCα and/or 1 mmol/L ATP were incubated for 30 minutes at 37°C and were cross-linked and immunoprecipitated as described in Materials and Methods. Cross-linked proteins were resuspended in 100 μL of SDS-PAGE sample buffer and analyzed by SDS-PAGE, followed by Western blots against anti-RLIP76 IgG, anti-p53 IgG, and anti-PKCα IgG. Lanes 1 to 5 shows the control with preimmune IgG (lane 1); immunoprecipitated RLIP76 and p53 (lane 2); RLIP76, p53 and 1 mmol/L ATP (lane 3); RLIP76, p53, and PKCα (lane 4); and RLIP76, p53, PKCα, and 1 mmol/L ATP (lane 5; A). Immunohistochemical localization of RLIP76 and p53 in p53-mutant (SKN-BE2) and p53-normal (LAN-5) neuroblastoma cells. Red, rhodamine for RLIP76; green, FITC for p53; yellow overlay indicating colocalization (B).

Effect of transfection of p53 on RLIP76-mediated transport of glutathione conjugates of 4HNE and DOX

The effect of p53 on the transport function of RLIP76 was analyzed in reconstituted liposomes treated with increasing concentrations of p53. P53 caused a concentration-dependent decrease in the transport activity of RLIP76. Both the transport of glutathione conjugates of 4HNE (GSHNE) and DOX was decreased in the presence of p53 (Fig. 3A and B). In the immunoprecipitation studies, we noted an enhanced binding of p53 to RLIP76 in the presence of PKCα (Fig. 2A). Hence, we further analyzed the impact of PKCα on p53-mediated inhibition of RLIP76 drug transport. Cotreatment with PKCα significantly enhanced the p53-induced inhibition of RLIP76-mediated drug transport in liposomes. In accordance with previously published studies, PKCα in the presence of 1 mmol/L ATP activated the drug transport by RLIP76. P53 caused significant decline in both the basal and PKCα-stimulated transport function of RLIP76 (Fig. 3C). Also, p53 caused maximum inhibition of RLIP76 transport in the absence of PKCα, but not in the presence of PKCα. Thus, though PKCα stimulates the binding of p53 to RLIP76; functionally, it partially reverses the p53-induced inhibition of RLIP76 transport. Thus, PKCα and p53 have opposite effects on the function of RLIP76 with either of them being able to partially reverse the effect of other. This is significant because previous studies by others have established that malignant neuroblastoma cells express a high level of PKCα along with nMyc and treatment with retinoic acid, which induces maturation of neuroblastoma cells to normal neuronal phenotype causes a decline of PKCα levels (34). Thus, the loss-of-p53 tilts the balance toward enhanced multidrug resistance that is mediated by RLIP76 both due to overexpression of RLIP76 and uninhibited

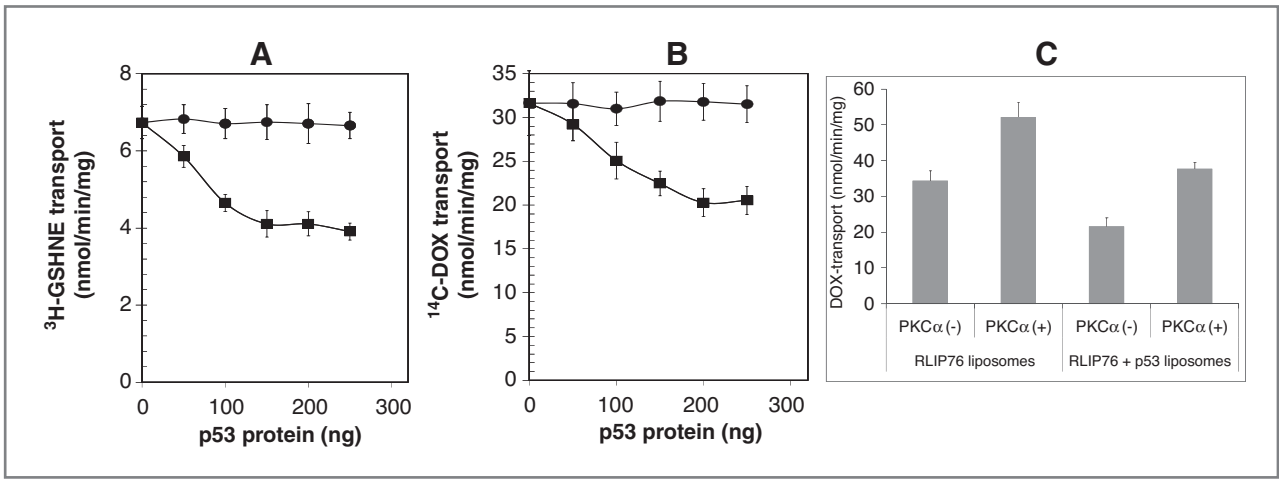

Figure 3. Effect of p53 and PKCα on the transport activity of RLIP76. The transport activity of RLIP76 toward GSHNE (A) and DOX (B) was measured by using purified rec-RLIP76 reconstituted into artificial cholesterol/asolectin liposomes as previously described (24). The effect of p53 (squares) or bovine albumin serum (round dots) at varying molar ratios was examined by incubating varying concentrations of these proteins in the transport medium. Transport medium contained RLIP76 proteoliposomes (250 ng protein/30 μL reaction mixture), 10 μmol/L ^{3}H-GSHNE (specific activity, 3.1×10^4 cpm/nmol), or 3.6 μmol/L ^{14}C-DOX (specific activity, 8.5×10^4 cpm/nmol), without or with 4 mmol/L ATP (3 experiments, each in triplicate; $n = 9$). Heat-inactivated p53 protein was also used for additional control. The effect of p53 on PKCα-stimulated ^{14}C-DOX transport activity of RLIP76 was also carried out (C). RLIP76 liposomes alone or in combination with p53 liposomes were divided into 4 groups for preincubation for 30 minutes at 37°C: first and third, 1 mmol/L ATP and no PKCα; second and fourth, 1 mmol/L ATP and 0.05 μg PKCα/μg of liposome. In first and second, RLIP76 liposomes were used, and in third and fourth, a mixture of RLIP76 + p53 liposomes was used. Transport assay was then carried out in the established manner by addition of proteoliposomes (RLIP76 or RLIP76 + p53, 250 ng each in 30 μL reaction mixture per filtration well, in triplicates) to transport buffer containing 3.6 μmol/L ^{14}C-DOX and either 0 or 4 mmol/L ATP. ATP-dependent transport was calculated by subtracting uptake in the absence of ATP from that in the presence of 4 mmol/L ATP. Results are average and SD from 3 separate experiments, each in triplicates ($n = 9$).

stimulation of drug transport by RLIP76 by activators such as PKCα in advanced neuroblastomas.

RLIP76 inhibition induces cell death and enhances CDDP sensitivity in neuroblastoma

We further investigated the effect of inhibition of RLIP76 by using antibodies and antisense. Depletion of RLIP76 by antisense increased the cell death in neuroblastoma cells (Fig. 4A). RLIP76 inhibition substantially enhanced the sensitivity to CDDP in both p53-mutant neuroblastoma cell lines and those expressing wild-type p53 (Fig. 4B; $P < 0.01$). The marginally enhanced susceptibility of p53 wild-type SMS-KCNR and LAN-5 neuroblastoma cells to RLIP76 antisense–induced cell death

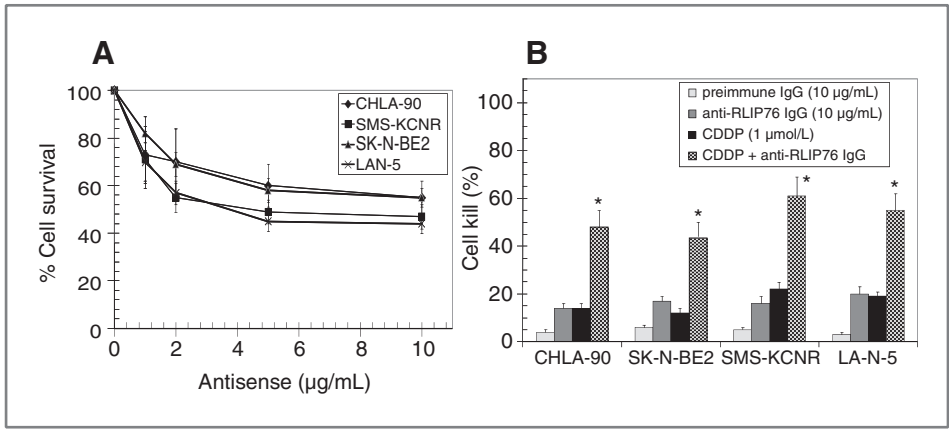

Figure 4. A, dose-dependent cytotoxicity induced by RLIP76 antisense (R508) in neuroblastoma cells. Cells were treated with R508 by using Maxfect transfection reagent (MoleculA, Inc.). Cell survival was measured by MTT cytotoxicity assay 48 hours after treatment. The values are presented as mean ± SD from 2 separate determinations with 8 replicates each ($n = 16$). B, cytotoxic interactions of anti-RLIP76 IgG and CDDP. Cytotoxic effects were calculated for absorbance values obtained from MTT cytotoxicity assays. Cells were treated alone or in combinations with anti-RLIP76 IgG (10 μg/mL) and CDDP (1 μmol/L) for 48 hours before MTT assay. Eight replicates were done in 3 separate experiments ($n = 24$); *, $P < 0.01$.

and potentiation of CDDP toxicity may be due to the activation of alternate p53-dependent apoptotic pathways consequent to RLIP76 depletion-induced oxidative stress and enhanced intracellular drug concentrations in a p53 wild-type background. But, the substantial cell death in p53-mutant neuroblastoma cell lines reflects the ability of RLIP76 depletion alone to induce cell death, which, along with the RLIP76 inhibition–induced increase in drug sensitivity in p53-null background, is of specific relevance in the control of aggressive and drug-resistant p53-null neuroblastomas.

RLIP76 inhibition alone causes tumor regression in mice xenografts of neuroblastoma

The novel finding that RLIP76 depletion alone using antisense was effective in targeting neuroblastomas lead to further investigations. Both the p53-mutant CHLA-90 and SKN-BE2 cell lines did not form tumors in mice xenografts. Hence, we tested the impact of RLIP76 inhibition on mice xenografts of SMS-KCNR cells. A total of 2×10^6 neuroblastoma cells were injected in 100 μL PBS into subcutaneous flank of each nu/nu mice and tumors were allowed to develop. Approximately at day 30, when the tumors reached approximately 40 mm^2 the mice were treated with 200 μg of RLIP76 antibodies or antisense in 100 μL of PBS, and tumor growth was observed everyday by measuring the tumor cross-sectional area by using calipers. The RLIP76 inhibition alone, either by using antibody or antisense caused significant tumor regression (Fig. 5A). The average weight of tumors of treated mice was substantially less than that of the controls (tumor weight at day 44: control, 1.88 g; RLIP76 antibody or antisense treated, 0.39 g; Fig. 5B and C; $P < 0.001$). There was no loss in the weight of treated mice when compared with controls, which ruled out any dose-limiting overt off-target cytotoxicity consequent to RLIP76 inhibition. This confirmed the ability of RLIP76 inhibition to

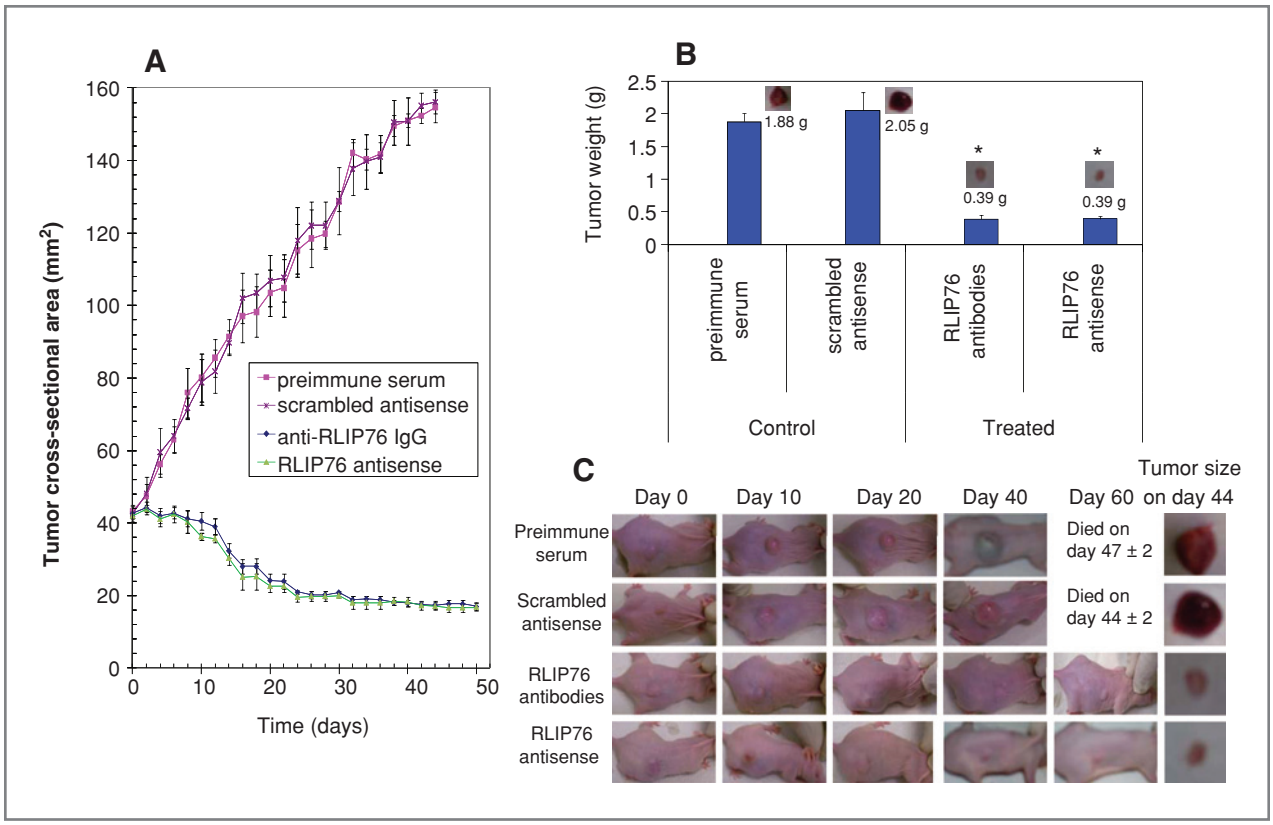

Figure 5. Effect of anti-RLIP76 IgG and RLIP76 antisense on the size of subcutaneously implanted human neuroblastoma cells in nude mice. Twenty 11-week-old nu/nu mice were divided into 4 groups of 5 animals (treated with preimmune serum, scrambled antisense DNA, anti-RLIP76 IgG, and RLIP76 antisense). All 20 animals were injected with 2×10^6 neuroblastoma cells (SMS-KCNR) suspensions in 100 μL of PBS, subcutaneously into 1 flank of each nu/nu nude mouse. Animals were examined daily for signs of tumor growth. When tumors reached a cross-sectional area of approximately 40 mm^2 (~30 days later), animals were randomized treatment groups as indicated in the figure. Treatment consisted of 200 μg of RLIP76 antibodies or antisense in 100 μL PBS, i.p. Control groups were treated with 200 μg/100 μL preimmune serum or scrambled antisense DNA. Tumors were measured in 2 dimensions by using calipers. Photographs of animals, taken at day 0, day 10, day 20, day 40, and day 60 after treatment, are shown for all groups. Tumor weights and photographs of tumors were also taken at day 44 after treatment. Tumor cross-sectional area in control and experimental groups (A and C); Tumor weight at day 44 (B and C). *, $P < 0.001$; $n = 5$.

successfully induce neuroblastoma tumor regression. Though, p53-mutant neuroblastomas did not develop tumors in mice xenograft studies, the significant efficacy of RLIP76 inhibition or depletion in p53-normal neuroblastoma was a striking finding for the ability to target RLIP76 alone in neuroblastomas. Taken together, our mice xenograft studies in p53-normal neuroblastomas along with the preceding drug transport studies where p53 inhibits RLIP76 and cell survival studies where RLIP76 is effective to a greater extent in p53-mutant neuroblastoma cell lines, the current research findings provide strong mechanistic and biological rationale for targeting RLIP76 in both p53-normal and p53-mutant neuroblastomas to achieve effective therapeutic response.

Discussion

Neuroblastomas are the most aggressive form of neuroblastic tumors with ganglioneuroblastoma and ganglioneuroma being the other succeeding aggressive tumors originating from the neural crest cells. Neuroblastomas have a median age of onset at 23 months and cause approximately 15% of the total cancer deaths in pediatric population. The neuroblastomas diagnosed before 18 months have good prognosis and many cases show spontaneous regression even without any clinical interventions. But, the survival of neuroblastomas incident after 18 months of age is poor at 42% (35). The neuroblastomas that occur in adolescents represent immense challenge to current interventions and are highly fatal (36). Approximately 60% of neuroblastomas present with metastases at different organs such as liver, bone-marrow, and cortical bones at the time of presentation, which limits localized surgical approaches and necessitates aggressive and effective chemotherapeutic interventions to achieve complete cure (37). Thus, targeting drug-resistant and relapsed tumors represents a contemporary focus of management in neuroblastomas.

Amplification of nMyc is an established cause in primary neuroblastomas, but nMyc is positively associated with aggressive course of disease in children ages more than 1 year at the time of diagnosis but not in infants (38–40). Treatment of neuroblastoma cells with cyclophosphamide induces apoptotic response by activating p53-dependent transcription of apoptotic genes such as *PUMA* and activation of proapoptotic proteins bax, bim, caspase 3, and caspase 9. P53-mediated apoptotic pathway is frequently altered in multidrug-resistant and relapsed neuroblastomas due to several causative factors (41). The nMyc amplification leads to attenuation of p53 function by stimulating the overexpression of p53 inhibitor Mdm2 (42).

Loss-of-function mutations in p53 lead to overexpression and uninhibited action of RLIP76 which contributes to chemoresistance. The p53-mutant neuroblastomas have enhanced levels of oxidative stress as revealed by increased concentration of 4HNE and MDA. Previous studies from our laboratory have shown that increased oxidative stress stimulates the expression of RLIP76 in K562 cells (43). Thus, p53-mutant neuroblastomas could be activating the transcription of RLIP76 as a stress-responsive protein to defend against toxic effects of enhanced oxidative stress. It is also possible that p53 could have a direct transcriptional role in regulating the expression of RLIP76. In this regard, the exact mechanisms that contribute to overexpression of RLIP76 in p53-mutant neuroblastomas need to be investigated further.

In addition to enhancing the chemosensitivity of coadministered drugs such as CDDP, RLIP76 alone represents a highly significant therapeutic target in multidrug-resistant neuroblastomas. Inhibition of RLIP76 alone induced significant cell death, which was more pronounced in p53-mutant neuroblastomas. Overexpression of RLIP76 in p53-mutant cancers itself could be a major pathogenetic factor for aggressive and metastatic neuroblastomas. In addition to its fundamental role in efflux of GS-E of lipid peroxidation products and chemotherapy drugs, RLIP76 regulates a spectrum of signaling events in cancer cells that are of importance in proliferation and metastases (Fig. 6). CDK1 binds to RLIP76 and translocates it to nucleus where it mediates the separation of chromosomal spindles during mitosis (44). PKCα-mediated proliferation and drug resistance require RLIP76 (29). RLIP76, through its RhoGAP domain, directly binds to and mediates adhesion-dependent activation of the GTPase R-Ras, leading to enhanced cell motility that was mediated by downstream Rac activation (45). RLIP76 is also negatively regulated by previously known inhibitors such as HSF-1, POB-1, and CDC2 (46, 47). P53, as evident from our current studies, is a novel inhibitor and arguably the most significant inhibitor in the context of multidrug resistance associated with loss-of-p53 in multiple malignancies. Most importantly, RLIP76 inhibition in our previous tumor models of mice did not reveal any deficits in the CNS functions and the experimental mice were active and normal without any loss of weight (48–50).

In summary, RLIP76 is a potential target for therapeutic interventions in refractory and relapsed neuroblastomas. In addition to well-defined nuclear and mitochondrial mechanisms of initiating p53-mediated apoptosis, for the first time, our results have established a novel "cell membrane" mechanism, in which active p53 inhibits the multidrug transporter RLIP76 to initiate a cascade of cell-death events that are mediated by an increase in intracellular concentration of ROS to toxic levels along with enhancing the intracellular concentration of administered chemotherapy drugs. The observed absence of off-target cytotoxicity as evident from our previous studies in RLIP76-targeted mice further corroborates the relevance of RLIP76-targeted chemotherapy for pediatric neuroblastomas, as such intervention would not compromise the normal growth and development of treated children. Thus, RLIP76 represents a novel and effective therapeutic target to treat multidrug-resistant neuroblastomas.

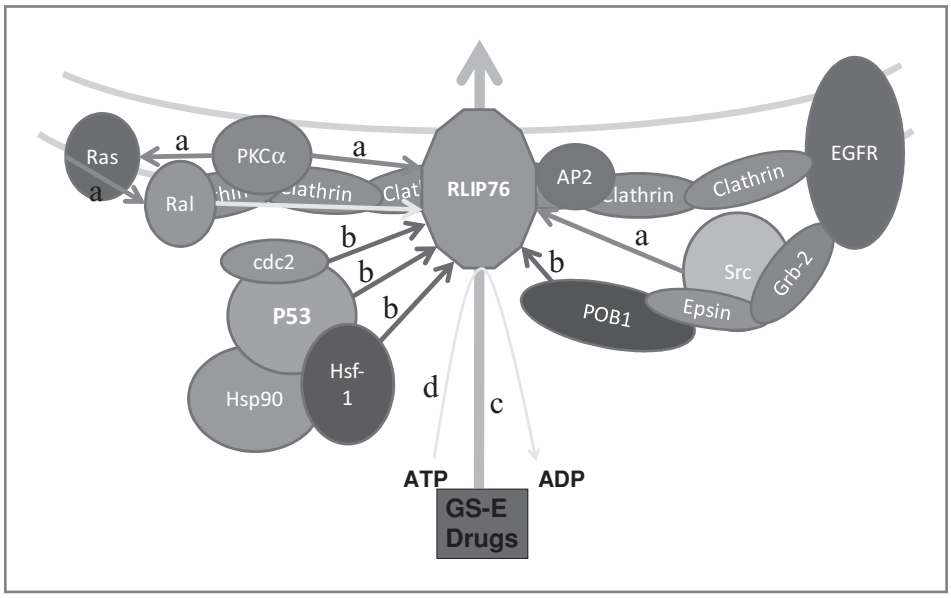

Figure 6. RLIP76: A multi-specific regulator of multi-drug resistance and tumor-progression: RLIP76 transports the GS-E of lipid-peroxidation products and administered chemotherapy drugs out of cells, thereby reducing the cytotoxic impact of both radiotherapy and chemotherapy. In addition, RLIP76 regulates vital proliferative and metastatic signaling networks in cancer cells (Arrows: "a"-stimulation; "b"-inhibition; "c"-transport and "d"-interaction). RLIP76 by its interaction with AP2 regulates the EGFR endocytosis. RLIP76 binds with CDK1 and translocates where it participates in the spindle formation during mitosis. RLIP76 is a critical mediator of PKCα-induced proliferation and drug resistance. RLIP76 enhances the migration of cells by activating GTPase R-Ras and Rac.

Disclosure of Potential Conflicts of Interest

No potential conflicts of interest were disclosed.

Acknowledgments

We thank Dr. Xiangle Sun, core facility at the University of North Texas Health Science Center, Fort Worth, TX, for helping with flow cytometry and laser capture microdissection (supported by NIH Grant ISIORR018999-01A1). We also thank Dr. Sumihiro Suzuki, Department of Biostatistics, School of Public Health, University of North Texas Health Science Center, Fort Worth, TX, for his assistance in the statistical analyses of the data.

Grant Support

This work was supported in part by USPHS grant CA 77495 (S. Awasthi and S.S. Singhal), the Cancer Research Foundation of North Texas (S.S. Singhal and S. Yadav) and Institute for Cancer Research and the Joe & Jessie Crump Fund for Medical Education (S.S. Singhal).

The costs of publication of this article were defrayed in part by the payment of page charges. This article must therefore be hereby marked *advertisement* in accordance with 18 U.S.C. Section 1734 solely to indicate this fact.

Received January 14, 2011; revised February 8, 2011; accepted February 28, 2011; published OnlineFirst March 16, 2011.

References

1. Berthold F, Hero B. Neuroblastoma: current drug therapy recommendations as part of the total treatment approach. Drugs 2000;59:1261–77.
2. Jacob ES, Varghese RG, Toi PC, Bhaskaran R, Rai R. Congenital neuroblastoma with liver metastasis presenting with Hashimoto Pritzker disease. Ind J Pathol Microbiol 2009;52:374–6.
3. DuBois SG, Kalika Y, Lukens JN, Brodeur GM, Seeger RC, Atkinson JB, et al. Metastatic sites in stage IV and IVS neuroblastoma correlate with age, tumor biology, and survival. J Pediatr Hematol Oncol 1999;21:181–9.
4. Smith SJ, Diehl N, Leavitt JA, Mohney BG. Incidence of pediatric Horner syndrome and the risk of neuroblastoma: a population-based study. Arch Ophthalmol 2010;128:324–29.
5. Wei JS, Greer BT, Westermann F, Steinberg SM, Son CG, Chen QR, et al. Prediction of clinical outcome using gene expression profiling and artificial neural networks for patients with neuroblastoma. Cancer Res 2004;64:6883–91.
6. Hawkes WC, Alkan Z. Regulation of redox signaling by selenoproteins. Biol Trace Elem. Res 2010;134:235–51.
7. Children's Oncology Group (CCG 09709),Khan J, Villablanca JG, Krailo MD, Ames MM, Reid JM, Reaman GH, et al. Phase I trial of oral fenretinide in children with high-risk solid tumors: a report from the Children's Oncology Group (CCG 09709). J Clin Oncol 2006;24:3423–30.
8. Garaventa A, Luksch R, Lo Piccolo MS, Cavadini E, Montaldo PG, Pizzitola MR, et al. Phase I trial and pharmacokinetics of fenretinide in children with neuroblastoma. Clin Cancer Res 2003;9:2032–39.
9. Fong A, Park JR. High-risk neuroblastoma: A therapy in evolution. Pediatr Hematol Oncol 2009;26:539–48.
10. Kubota M, Okuyama N, Hirayama Y, Asami K, Ogawa A, Watanabe A. Mortality and morbidity of patients with neuroblastoma who survived for more than 10 years after treatment—Niigata Tumor Board Study. J Pediatr Surg 2010;45:673–77.
11. Modak S, Cheung NK. Neuroblastoma: therapeutic strategies for a clinical enigma. Cancer Treat Rev 2010;36:307–17.
12. Seeger RC, Reynolds CP. Treatment of high-risk solid tumors of childhood with intensive therapy and autologous bone marrow transplantation. Pediatr Clin North Am 1991;38:393–424.

13. Manhani R, Cristofani LM, Odone Filho V, Bendit I. Concomitant p53 mutation and MYCN amplification in neuroblastoma. Med Pediatr Oncol 1997;29:206–7.
14. Keshelava N, Zuo JJ, Chen P, Waidyaratne SN, Luna MC, Gomer CJ, et al. Loss of p53 function confers high-level multidrug resistance in neuroblastoma cell lines. Cancer Res 2001;61:6185–93.
15. Houldsworth J, Xiao H, Murty VV, Chen W, Ray B, Reuter VE, et al. Human male germ cell tumor resistance to cisplatin is linked to TP53 gene mutation. Oncogene 1998;16:2345–9.
16. Lee JM, Bernstein A. P53 mutations increase resistance to ionizing radiation. Proc Natl Acad Sci U S A 1993;90:5742–6.
17. Amaral JD, Xavier JM, Steer CJ, Rodrigues CM. The role of p53 in apoptosis. Discov Med 2010;45:145–52.
18. Keshelava N, Zuo JJ, Waidyaratne NS, Triche TJ, Reynolds CP. P53 mutations and loss of P53 function confer multidrug resistance in neuroblastoma. Med Pediatr Oncol 2000;35:563–8.
19. Awasthi S, Singhal SS, Sharma R, Zimniak P, Awasthi YC. Transport of glutathione-conjugates and chemotherapeutic drugs by RLIP76 (RALBP1): a novel link between G-protein and tyrosine kinase signaling and drug resistance. Int J cancer 2003;106:635–46.
20. Vatsyayan R, Lelsani P, Awasthi S, Singhal SS. RLIP76: a versatile transporter and an emerging target for cancer therapy. Biochem Pharmacol 2010;79:1699–705.
21. Chesler L, Goldenberg DD, Collins R, Grimmer M, Kim GE, Tihan T, et al. Chemotherapy-induced apoptosis in a transgenic model of neuroblastoma proceeds through p53 induction. Neoplasia 2008;10: 1268–74.
22. Erster S, Mihara M, Kim RH, Petrenko O, Moll UM. In vivo mitochondrial p53 translocation triggers a rapid first wave of cell death in response to DNA damage that can precede p53 target gene activation. Mol Cell Biol 2004;24:6728–41.
23. Keshelava N, Seeger RC, Groshen S, Reynolds CP. Drug resistance patterns of human neuroblastoma cell lines derived from patients at different phases of therapy. Cancer Res 1998;58:5396–405.
24. Awasthi S, Cheng J, Singhal SS, Saini MK, Pandya U, Pikula S, et al. Novel function of human RLIP76: ATP-dependent transport of glutathione-conjugates and doxorubicin. Biochemistry 2000;39:9327–34.
25. Sharma R, Singhal SS, Cheng J, Yang Y, Sharma A, Zimniak P, et al. RLIP76 is the major ATP-dependent transporter of glutathione-conjugates and doxorubicin in human erythrocytes. Arch Biochem Biophys 2001;391:171–9.
26. Aumais JP, Lee HS, Lin R, White JH. Selective interaction of hsp90 with an estrogen receptor ligand-binding domain containing a point mutation. J Biol Chem 1997;272:12229–35.
27. Awasthi S, Singhal SS, Pikula S, Piper JT, Srivastava SK, Torman RT, et al. ATP-dependent human erythrocyte glutathione-conjugate transporter. II. Functional reconstitution of transport activity. Biochemistry 1998;37:5239–48.
28. Yadav S, Singhal SS, Singhal J, Wickramarachchi D, Knutson E, Albrecht TB, et al. Identification of membrane-anchoring domains of RLIP76 using deletion mutant analyses. Biochemistry 2004;43: 16243–53.
29. Singhal SS, Yadav S, Singhal J, Drake K, Awasthi YC, Awasthi S. The role of PKCα and RLIP76 in transport-mediated doxorubicin-resistance in lung cancer. FEBS Lett 2005;579:4635–41.
30. Bensaad K, Vousden KH. Savior and slayer: the two faces of p53. Nat Med 2005;11:1278–9.
31. Dwivedi S, Sharma A, Patrick B, Sharma R, Awasthi YC. Role of 4-hydroxynonenal and its metabolites in signaling. Redox Rep 2007; 12:4–10.
32. Lee YS, Wan J, Kim BJ, Bae MA, Song BJ. Ubiquitin-dependent degradation of p53 protein despite phosphorylation at its N terminus by acetaminophen. J Pharmacol Exp Ther 2006;317:202–8.
33. Bardag-Gorce F, French BA, Nan L, Song H, Nguyen SK, Yong H, et al. CYP2E1 induced by ethanol causes oxidative stress, proteasome inhibition and cytokeratin aggresome (mallory body-like) formation. Exp Mol Pathol 2006;81:191–201.
34. Tonini GP, Parodi MT, Di Martino D, Varesio L. Expression of protein kinase C-alpha (PKC-alpha) and MYCN mRNAs in human neuroblastoma cells and modulation during morphological differentiation induced by retinoic acid. FEBS Lett 1991;280:221–4.
35. London WB, Castleberry RP, Matthay KK, Look AT, Seeger RC, Shimada H, et al. Evidence for an age cutoff greater than 365 days for neuroblastoma risk group stratification in the children's oncology group. J Clin Oncol 2005;23:6459–65.
36. Franks LM, Bollen A, Seeger RC, Stram DO, Matthay KK. Neuroblastoma in adults and adolescents: an indolent course with poor survival. Cancer 1997;79:2028–35.
37. DuBois SG, Kalika Y, Lukens JN, Brodeur GM, Seeger RC, Atkinson JB, et al. Metastatic sites in stage IV and IVS neuroblastoma correlate with age, tumor biology, and survival. J Pediatr Hematol Oncol 1999;21:181–9.
38. Weiss WA, Aldape K, Mohapatra G, Feuerstein BG, Bishop JM. Targeted expression of MYCN causes neuroblastoma in transgenic mice. EMBO J 1997;16:2985–95.
39. Fulda S, Lutz W, Schwab M, Debatin KM. MycN sensitizes neuroblastoma cells for drug-induced apoptosis. Oncogene 1999;18: 1479–86.
40. Bordow SB, Norris MD, Haber PS, Marshall GM, Haber M. Prognostic significance of MYCN oncogene expression in childhood neuroblastoma. J Clin Oncol 1998;16:3286–94.
41. Carr J, Bell E, Pearson AD, Kees UR, Beris H, Lunec J, et al. Increased frequency of aberrations in the p53/MDM2/p14(ARF) pathway in neuroblastoma cell lines established at relapse. Cancer Res 2006;66: 2138–45.
42. Slack A, Chen Z, Tonelli R, Pule M, Hunt L, Pession A, et al. The p53 regulatory gene MDM2 is a direct transcriptional target of MYCN in neuroblastoma. Proc Natl Acad Sci 2005;102:731–6.
43. Cheng JZ, Sharma R, Yang Y, Singhal SS, Sharma A, Saini MK, et al. Accelerated metabolism and exclusion of 4-hydroxynonenal through induction of RLIP76 and hGST5.8 is an early adaptive response of cells to heat and oxidative stress. J Biol Chem 2001;276:41213–23.
44. Rosse C, L'Hoste S, Offner N, Picard A, Camonis J. RLIP, an effector of the ral GTPases, is a platform for Cdk1 to phosphorylate epsin during the switch off of endocytosis in mitosis. J Biol Chem 2003;278:30597–604.
45. Jullien-Flores V, Dorseuil O, Romero F, Letourneur F, Saragosti S, Berger R, et al. Bridging ral GTPase to rho pathways. RLIP76, a ral effector with CDC42/Rac GTPase-activating protein activity. J Biol Chem 1995;270:22473–7.
46. Singhal SS, Yadav S, Vatsyayan R, Chaudhary P, Borvak J, Singhal J, et al. Increased expression of cdc2 inhibits transport function of RLIP76 and promotes apoptosis. Cancer Lett 2009;283:152–8.
47. Singhal SS, Yadav S, Drake K, Singhal J, Awasthi S. Hsf-1 and POB1 induce drug sensitivity and apoptosis by inhibiting Ralbp1.J Biol Chem 2008;283:19714–29.
48. Singhal SS, Awasthi YC, Awasthi S. Regression of melanoma in a murine model by RLIP76 depletion. Cancer Res 2006;66:2354–60.
49. Singhal SS, Singhal J, Yadav S, Dwivedi S, Boor PJ, Awasthi YC, et al. Regression of lung and colon cancer xenografts by depleting or inhibiting RLIP76 (ral-binding protein 1). Cancer Res 2007;67:4382–9.
50. Singhal SS, Singhal J, Yadav S, Sahu M, Awasthi YC, Awasthi S. RLIP76: a target for kidney cancer therapy. Cancer Res 2009;69: 4244–51.